

Dear Editor and reviewers,

We would like to thank the two anonymous reviewers and yourself for the feedback on our manuscript. We have addressed point-by-point both the major and minor points raised by the reviewers below. We have addressed all comments and suggestions, and have implemented the vast majority of them in the updated manuscript. We believe this has improved the manuscript quality. We hope that you find our response satisfactory and see that our dataset and manuscript as a good fit for the ESSD journal.

Kind regards,  
Jenny Turton, Thomas Mölg and Emily Collier.

### Response to Reviewer 1

1: The open-source numerical simulation model (Polar WRF) itself is not developed by the authors. In my opinion, it implies that anyone who has enough scientific budgets can do this kind of numerical simulations relatively easily, so that the data lack high level originality. *Whilst we agree with the reviewer that we do not develop the model, and also that, due to its open source and well documented nature many people can use WRF, we do not think that this detracts from the novelty of the manuscript. If we were to develop the model, or aspects of it, the results would likely be published in a model development journal, as opposed to a data journal. This dataset meets the aims of the journal in that high-quality data can be reused at a benefit to the earth system science community. Furthermore, we have conducted sensitivity studies and worked with the WRF model for over a decade, which means we are able to simulate this complex region using the most appropriate physics options (of which there are hundreds of combinations and many which would not be applicable or justifiable in the polar regions) as opposed to the default values which have unfortunately been used in many papers incorrectly. Furthermore, conducting these model runs at such a high spatial and temporal resolution took a large amount of computer time and money, which many colleagues in the scientific community do not have direct access to. Published papers within the ESSD journal include the use of ERA5 or other reanalysis products which are available online, and output from other models which were not developed by the authors, therefore we believe our paper to be within scope of this journal.*

2: The authors do not validate the D3 model simulation results in terms of downward shortwave and longwave radiations, as well as surface (snow and ice) mass balance. Because downward radiations and precipitation are very important input parameters for hydrological and oceanic models, their argument “the dataset can be used to input for hydrological and oceanic modelling studies” is not supported by any objective evidence. Please note almost no direct precipitation measurement data on the Greenland ice sheet are available, so, usually, polar regional climate models are validated in terms of surface mass balance to confirm the models’ performance simulating precipitation.

*Thank you for this comment. We have now included a validation of the downward shortwave and longwave radiations as suggested, in table 2 and in section 3.1 of the results. We refrain from including any mass balance analysis or validation, as there is an ongoing project which is using the atmospheric WRF data as input to a mass balance model and will include a comparison to the WRF data. Please also see our response to P5 L 121-122 (about the*

*snowpack), as it is relevant here. Furthermore, we have added the following “subject to appropriate validation” to the manuscript when referencing the datasets potential uses (Line 392).*

### Major Comments

P. 1, L. 17 ~ 19: In order to argue “The dataset, (Turton et al, 2019b: doi.org/10.17605/OSF.IO/53E6Z), is now available for a wide variety of applications ranging from atmospheric dynamics, to input for hydrological and oceanic modelling studies”, the authors should show model validation results in terms of downward shortwave and longwave radiations as well as surface mass balance.

*Thank you for the comment. We have included a validation of the results for downward shortwave and longwave radiation and agree that it is useful for future users. See Table 2 and lines 256 to 272.*

P. 2, L. 44: However, recently, there are several attempts that applying high-resolution non-hydrostatic polar regional climate models in Greenland (Mottram et al., 2017; Niwano et al., 2018).

*Thank you for highlighting this missing information. We have now included the following sentence: “Recently, there have been attempts at modelling the polar regions using non-hydrostatic regional climate models, including HARMONIE-AROME at 2 km resolution for the Southwest of Greenland (Mottram et al 2017b), and the NHM-SMAP at 5 km resolution for the whole of Greenland (Niwano et al 2018). However, the Mottram et al (2017b) study does not include the northeast of Greenland. Furthermore, the focus of the Niwano et al (2018) study was to improve the surface mass balance estimates, as opposed to providing output for a more general atmospheric sense, and the model was not convection permitting”. (line 69-75).*

P. 2, L. 46: I think this model simulation by the authors is not “novel”, because the model itself is not developed by the authors, which implies that anyone who has enough scientific budgets can do this kind of numerical simulations relatively easily.

*Please see our response to the major questions above. However, we have removed the word novel here, as it does not alter the sentence, nor the impact of the paper.*

Table 1: As far as I know, T2, Q2, WS10, and WD10 are not provided by GEUS. The provided T, Q, WS, and WD data are affected by surface height changes through accumulation/ablation. *Yes, you are right. We have now altered table 1 and the citation to reflect this. Furthermore, we have added in a number of sentences in section 2.2 to explain our convention. This section now reads as: “Observations are not measured at exactly 2m above the surface but vary with accumulation and ablation. Over bare ice, the sensor is 2.6m above the surface (van As et al. 2011). To clarify that the observations represent near-surface conditions, and are compared with 2m and 10m model output, we use the abbreviation X2 or X10 to represent both modelled and observed variables at the respective heights.” (line 205-209).*

Table 2: Please indicate coefficient of determination ( $R^2$ ) instead of correlation. For the model validation, indicating the  $R^2$  value is more general in my opinion.

*Thank you for your comment. This has now been changed in Table 2 and throughout the manuscript.*

Sect. 3.2: Why not directly showing comparison results for 1hour data?

*We are only comparing the WRF data with observations for the purpose of highlighting its skill and weaknesses for future users. We advise that any future users validate the model output for their own purposes and in a more detailed manner, therefore we chose only to show daily averages. To provide some information about the sub-daily skill, we discuss the diurnal temperature cycle and min/max values only.*

#### Minor comments

P. 1, L. 15: It is better to indicate time resolution here as well.

*Included. The section now reads: "Here we present a high spatial- (1 km) and temporal- (up to hourly) resolution atmospheric modelling dataset." (line 19).*

P. 2, L. 53: I think katabatic winds and warm-air advection can be simulated accurately even by a 5 km non-hydrostatic atmospheric model if the model considers detailed atmospheric and snow/ice physical processes in an appropriate manner.

*Yes, we agree, as the warm-air advection processes can be seen in our 5km output too, but of course with less detail around the complex topography. We have altered the sentence to highlight that less than 5km would be good for these processes, and to include suggestions from reviewer 2. It reads as: "With a horizontal resolution of less than 5km, many atmospheric processes are accurately resolved including katabatic winds and warm-air advection (Turton et al., 2019a). Furthermore, high-resolution output is crucial for the complex topography on the northeast coast, where steep and variable topography can channel or block the winds, and lead to strong variability of the radiation budget." (Line 87-90)*

P. 2, L. 54 ~ 55: Which model configurations (D1 ~ D3) can be used for this purpose? Please explain more.

*We have not included these changes, as the domains have not yet been introduced.*

P. 4, L. 83: What are the "other sources"? Please specify them.

*Compared to MERRA2 reanalysis specifically, which has now been included. In Turton et al 2019a, we compared ERA Interim and MERRA2 to observations and found that ERA Interim was the more accurate choice. We only looked at ERA Interim and MERRA2 based on a study by Reeves-Eyre and Zeng (2017), who found these two to be the most accurate for our study area. This section now reads as: "This reanalysis product was more accurate at resolving mesoscale processes in the northeast of Greenland compared to MERRA2 reanalysis data and has previously been used to initialise WRF in this region (Turton et al., 2019a)." (line 118).*

P. 4, L. 109: Please explain why the Kain-Fritsch cumulus convection parameterization scheme was applied only for the D1 and D2 configurations.

*From the literature and experience of the mesoscale modelling community, resolutions as coarse as 4km can be sufficient to resolve convection explicitly in non-hydrostatic models but resolutions of 1km give the most confidence in results (Weisman et al 1997). Resolutions*

*between 8 and 12km can resolve convective processes only partly and often with timing issues, so parameterisation is recommended (Weisman et al 1997). Depending on which literature is assessed, anywhere between 2 and 20km is the 'grey area', and there is contrasting evidence in regard to whether one should or shouldn't use a parameterisation in this resolution range. We opted to use it based on previous studies and sensitivity analysis which showed little difference in output if the parameterisation scheme was or wasn't applied. This sentence has been altered to better reflect this information: "Further parameterisations include: the Kain-Fritsch scheme for cumulus convection (Kain, 2004) (D01 and D02 only, as the 1 km resolution of D03 allows convection to be explicitly resolved)." (Line 160).*

P. 5, L. 121~ 122: For snowpack, how deep do the authors consider in the model? Also, how did the authors confirm "the snowpack was adequately spun up before the onset of the accumulation season"?

*The model was spun up during September, when there is typically no snow left on the glacier and bare ice is visible (from observations), but any water on the glacier has started to freeze over. The snowpack is handled by the NOAA land surface model (Chen & Dudhia, 2001), with some improvements to better represent the polar regions in Polar WRF (Hines & Bromwich, 2008). Maximum snow depth at the location of the AWS stations is approx. 3m, in June 2018, a year that had a significantly larger snowfall than previous years, when looking at ERA5 data (Turton et al. in prep). We used the observations of snow depth further south (74°N) along the coast by Pedersen et al. (2016) to compare against NEGIS\_WRF runs in our D02 (during testing), which includes this location. In 2014 (the only year which overlaps with Pedersen's study), they record a max snow depth of approx. 0.9m in June 2014. At this location from NEGIS\_WRF, 0.8m was simulated. Typically, this location is drier than 79N due to the blocking topography.*

*Below the snowpack, the land surface model treats glacier areas as fully saturated and fully frozen soils (Chen & Dudhia, 2001., Hines & Bromwich, 2008). This is appropriate for NE Greenland due to the low temperatures at this location. However, this is a limitation of WRF in glacierised areas, and this is more of an issue in mid-latitude glacier settings (see Collier et al. 2015; doi:10.5194/tc-9-1617-2015 for details). It is well known that the glacierised processes in WRF are simplified (for example, densification is not included), which is another reason why the authors refrain from providing an evaluation of the WRF-simulated surface mass balance. Instead, a study is currently underway to force a SMB model with NEGIS\_WRF atmospheric data for this region to provide a more rigorous estimate of the SMB. As you mention above, there are little to no precipitation observations for this region. Wang et al (2019 :doi:10.5194/tc-13-1661-2019) compared ERA5 products with observations of precipitation from buoys in the Arctic sea ice (and near to the NE coast) and found a good agreement between ERA5 and observations in terms of snowfall. We have included the following line to highlight these changes: "The model produces similar magnitude snow depths to available observations (Pedersen et al. 2016). Due to limited snowfall and snow depth observations in this region, we compared cumulative snowfall to ERA5 products during testing, which have been shown to have a relatively good agreement with observations by Wang et al. (2019). The maximum snow depth and average annual accumulation were well captured by Polar WRF compared to ERA5" (line 175- 180).*

Technical corrections

Please unify notations of the model domains throughout the manuscript. At present, there are three types of notations like “d02”, “D02”, and “D2”.

*Thank you for pointing this out, we have now remained consistent with the D02 style of notation.*

Figure 1: Please indicate the NEGIS area in this map as well.

*This has now been included based on the Khan et al. (2014) study.*

## Response to Reviewer 2

Specific comments:

Still, I am missing one example plot (e.g. temperature map with wind arrows on top) of a comparison between the 1-km resolution WRF output for the 79 North Glacier region and existing atmospheric models (e.g., RACMO2 at 11 km).

*Thank you for this comment. We have now included an additional image (now called Figure 4) of the temperature and wind over the region, to highlight its skill in the spatial sense. We have decided not to compare with another model, as this would mean that we include another dataset only to compare for one figure, and we have attempted to keep comparison to other data and interpretation minimal to keep within the scope of the journal. We attempted to find published figures from atmospheric models for this region, but were unable to find some for a good comparison. We think that including the new figure (4) will provide readers with a sense of how much detail is provided in 1km resolution runs.*

1. Structure of the manuscript: - The subsection 2.3 seems rather short and redundant. The model evaluation is what is shown and described in detail in the following result sections. I would suggest to merge 2.2 and 2.3, i.e., describing briefly what you will use the observational data for, leading over to the result section. - You are lacking section 4. (Section 3 are the results and section 5 is the conclusion.) - To be more precise, I would suggest to change the subtitles of the result sections to sth like 3.1 Model evaluation: Daily-means 3.2 Model evaluation: Sub-daily data 2.

*Thank you for your suggestion. We have removed subsection 2.3, by incorporating the relevant information into section 2.2 and including some introductory sentences into the relevant results section (3). We have also changed the subtitles as you suggested. The numbering was wrong, as ‘data availability’ was numbered as 4, but actually came after section 5 (conclusions). We have now numbered them correctly.*

2. References/citations: Some references were not appropriate/missing.

Line 22: Schaffer et al 2017 cited similar content in their introduction but this is not the content of their paper. Furthermore, mass loss of the Greenland ice sheet increased not only due increased ice discharge along the margin of the ice sheet (linked to the retreat of marine terminating glaciers) but also due to increased surface melt. Please elaborate this a bit more and refer to recent publications (e.g., Shepherd, A., Ivins, E., Rignot, E. et al. Mass balance of the Greenland Ice Sheet from 1992 to 2018. Nature (2019) doi:10.1038/s41586-019-1855-2).

*Thank you for this suggestion. We have changed the Schaffer et al 2017 citation to one more specific (Howat and Eddy 2011). We have also included more description of the mass changes and included relevant information from the Shepherd et al publication. We have also shuffled some of the sentences around after including this information. The section now reads as: “The surface mass balance of a glacier is largely controlled by regional climate through varying mass gains and losses in the ablation and accumulation zones, respectively. The large amount of mass lost from the Greenland Ice Sheet (GrIS) within the last few decades (approximately 3800 billion tonnes of ice between 1992 and 2018: Shepherd et al., 2019) has largely been located around the coast of Greenland, due to the thinning and retreat of marine-terminating glaciers (Howat & Eddy, 2011), and the surface mass loss in the ablation zone due to enhanced melting and runoff (Rignot, et al., 2015; van den Broeke et al., 2017). A recent study found that enhanced meltwater run off, connected to changing atmospheric conditions, was the largest contributor of mass loss for Greenland (52%) (Shepherd et al., 2019). The remaining 48% of mass loss (1.8 billion tonnes of ice) was due to enhanced glacier discharge, which has been increasing over time (Shepherd et al., 2019).” (Line 27 – 36).*

Line 34: Is 1 m/yr given as an average melting over the entire glacier tongue? Thinning of the glacier tongue and its variability in time has been also discussed in Mayer et al 2018. Furthermore, Wilson et al 2017 (The Cryosphere) and Mayer et al 2018 point out that thinning is mainly due to enhanced melt along the glacier base. Thus, surface melt (triggered by atmospheric changes) seems to be of minor relevance. However, the atmosphere may be relevant e.g. for driving oceanic heat toward the glacier (Münchow et al 2018, accepted at Journal of Physical Oceanography) and below the glacier tongue. If there is space, you could include these information to point out the relevance of a better understanding of atmospheric conditions to study the observed changes at the 79°N Glacier.

*Thank you for these comments. We have now altered the sentence to better describe the thinning and the relevance of the ocean and atmosphere on melting. We have included more literature that you suggest, which provides more detail and explanation of the glacier. This section now reads as: “However, 79°N glacier, with its 80 km long by 20 km wide floating tongue, has retreated by 2-3km between 2009 and 2012, and the surface of the tongue and part of the grounded section of the glacier are now thinning at a rate of 1 m yr<sup>-1</sup> (Khan et al., 2014, Mayer et al. 2018). The glacier is at a crucial interface between a warming ocean and a changing atmosphere. The mass loss from the floating tongue is largely attributed to basal melting due to the presence of warm (1°C) ocean water in the cavity below the glacier (Wilson and Straneo 2015, Schaffer et al. 2017, Münchow et al. 2019). Even the grounded part of the glacier is characterised by large melt ponds and drainage systems (Hochreuther et al, in prep), suggesting atmospheric processes may also be at play. Furthermore, atmospheric processes may be responsible for driving the warm Atlantic water under the glacier tongue, which leads to melting of the glacier base (Münchow et al. 2019). 79°N glacier is of further interest because its southerly neighbour, Zachariae Istrom, recently lost its floating tongue (Mouginot et al., 2015).” (Line 46-48).*

Lines 36-39: I would suggest to compare/list atmospheric modelling studies only or make more clear what kind of models were used in the listed publications. Schaffer et al 2017 do not use model data.

*Yes we agree that this would be wiser, we have therefore limited it to atmospheric modelling studies only.*

Line 89: “Analysis nudging” – I am not a modeler, so I am not fully sure how common it is to use analysis nudging. I suggest to give a reference or add a very brief explanation on how this works.

*Thank you for this comment. We have now included a number of sentences and references to explain this briefly. This section now reads as: “Nudging is the process of constraining the interior of model domains towards the reanalysis data which drive the simulation (Lo et al. 2008., Otte et al. 2012). It has been found to improve simulations of the large-scale circulation (Bowden et al. 2012) and reduce errors in the mean and extreme values (Otte et al. 2012) from relatively long runs. We only nudge the outer domain (D01) to allow the higher-resolution domain to evolve freely.” (Line 131-135).*

### 3. Scientific questions/add-ons

Line 43-45: I suggest to point out why a 1-km resolution makes a difference in the coastal area of Greenland. One reason that you did not mention (or I missed it) is, that the topography along the coast is very steep and complex with a number of narrow fjords and small islands most likely channeling/blocking/steering the wind in your area of interest.

*Thank you. We have now included a sentence with this information. It reads as: “Furthermore, high-resolution output is crucial for the complex topography on the northeast coast, where steep and variable topography can channel or block the winds, and lead to strong variability of the radiation budget.” (Line 88-90).*

Line 88: Did one of the studies show that SST and sea ice concentration from the AVHRR compare well to other observations/satellite data?

*We have now included a little more description of the dataset and included a reference where readers can find out about validation of the data for different regions. This section now reads: “NOAA Optimum Interpolation 0.25° resolution daily data. This is a combination of data from the Advanced Very High Resolution Radiometer (AVHRR) infrared satellite and Advanced Microwave Scanning Radiometer (AMSR) (doi:10.5065/EMOT-1D34, data retrieved from <https://rda.ucar.edu/datasets/ds277.7/>, last accessed July 29 2019). In-situ ship and buoy data are used to correct satellite biases, leading to relatively low mean biases of 0.2-0.4K for SST data (more information on this dataset can be found in Banzon et al. 2016).” (Line 120-125).*

Lines 93-97: A map showing Spalte Glacier and marking the open-water grid points would certainly help to better understand what you are describing. Are you also referring to the fast-ice cover named Norske Øer Ice Barrier (Sneed and Hamilton, 2016, Annals of Glaciology) here? Furthermore, I would split this long sentence into two.

*Thank you for these suggestions. The sentence has been split and now reads as: “Other small exposed water areas along the coast, which are permanently frozen except in July and August each year (Hochreuther, P., 2019 personal communication), were also changed to ice during all months except July and August.” (Line 141-144).*

*We have changed Figure 2 based on suggestions from yourself and Reviewer 1. The revised figure shows the land-use properties of the inner domain, labels important regions and highlights the changed grid points. The sea ice concentration data is the only information*

*provided about the sea ice conditions. The resolution of the data is 0.25°, so will not include small polynyas, leads or ice breakup. The concentration of sea ice is much lower very close to 79N (0.1-0.4 fraction) and Zachariae than further north and east (0.8-1.0 fraction), which may represent the thin, fast ice of the ice barrier.*

Lines 97-98: “given the small area of calving at 79°N during this period.” – I understand what you like to say but I think you should be more precise. You are talking about a (negligible) area change caused from calving at/advancing of the glacier front. Furthermore, it is not clear to me which time period you are referring to. Please specify.

*The time period is during our study period, from 2014-2018. The text has been altered to make that clear. There is little information about the amount of area lost to calving during this time, but from looking at the shape files of glacier extent and calving front locations available at [cryoportal.enveo.at](http://cryoportal.enveo.at), it is clear that the area of change is negligible. This section now reads as: “The glacier extents are treated as static throughout the run, which is an appropriate approximation given the small and likely negligible area of calving of 79°N during our study period (see ENVEO, 2019 for calving front locations from 1990 to 2017).” (Line 145-146).*

Figure 2: Please add the shape (in white?) of the 79 North Glacier and point out its location. If possible, also add the location of Spalte Glacier and the approximate extent of the fast-ice cover. I believe that the dark blue color is missing in the Figure. At least I cannot distinguish areas deeper sea level from areas between 0 – 200 m height. Just from the color code, it looks like the islands along the coast are half under water.

*We have revised figure 2 to provide more information about the region in terms of land use and location names. We have included labels for 79N and Spalte glacier. The height contour information from the previous figure (now removed) has been included in Figure 4 (a new figure of the temperature and winds). Adding the shape of 79N is not fully possible, as there is no clear outline of the glacier other than its floating tongue. It joins the North East Greenland Ice Stream (NEGIS) along with 2 other glaciers, and therefore there is no clear outline of where 79N stops and NEGIS begins. We have chosen not to include the extent of the fast ice, as we do not discuss this in the paper, and it is not an additional data source in the model, but will only be represented by the sea ice concentration. Furthermore, this extent changes annually, and seasonally, which would make the plot quite complicated.*

Section 2.3: As stated above you may want to merge/skip this section. In case you keep it, I like to make you aware that it reads as if you compare air temperatures for model evaluation only, which is not the case.

*Thank you for this. We have now removed section 2.3 and merged the relevant parts into 2.2, but removed the part which made it seem like we only compared temperatures.*

4Table 2, Line 163: I am not fully sure what the correlation coefficient refers to. Do you correlate the time series from WRF and AWS data over the entire measurement period? What do you mean by “annual correlation”? Do you correlate the annual means, i.e., 5 time steps only?

*As suggested by Reviewer 1, we have now calculated the coefficient of determination ( $R^2$ ) rather than correlation coefficient, so the values have changed in table 2 and throughout the manuscript. For these calculations, we use daily averages of hourly observations and model*



*output from the entire study period from 2014-2018 for the 'ANN' values. This is what we meant by 'annual correlation'- data from throughout the years. As opposed to R2 values calculated only for DJF and JJA months. We see how this is misleading, so have changed the sentence slightly.*

Line 174: "is more variable" – better use sth like "deviates more from the ASW data". Is that maybe due to the very steep topography presumably not covered by your 1- km resolution? Please discuss throughout the whole manuscript what may cause the described errors. How big are errors in the wind direction measured at the automatic weather stations?

*Thank you for these suggestions. This sentence now reads as: "The wind direction in WRF deviates more from the AWS data than for temperature and moisture, which is likely due to the particularly steep and complex topography of the region which may not be accurately represented by the model at 1-km resolution." (Line 244-247).*

*We have now included more information on the errors throughout the manuscript. Table 1 now has an added column with information on the error from the automatic weather station sensors. We have now included information and discussion around the errors throughout the manuscript, which will appear in red text, but specifically, a sentence has been added in section 3.1 which says: "Some of these [wind direction] errors may relate to measurement errors of the wind sensor, which is +/-3° (see Table 1)." (Line 250-251).*

Line 178: "is simulated better" – better use "more accurate" or "the model performs better in simulating. . ." or give specific numbers

*Thank you. Changed to: "The model performs better at simulating the wind speed than the wind direction." (Line 251-252)*

Line 197: "WRF can simulate much higher wind speeds than observed" – Are these higher wind speeds (more) realistic? I am missing an interpretation/assessment/discussion of this result.

*Thank you for this suggestion. We avoided interpreting the results in detail, as this is out of the scope of this journal. However, we have now included some references to other literature. Higher simulated wind speeds from WRF, when compared to ERA Interim data (as we do here) were also found for the south east coast of Greenland by Duvivier & Cassano (2015).*

*Compared to ERA-Interim, these differences could arise due to the different treatment of snow- and ice-covered surfaces and sea ice between WRF and the model used in ERA Interim. These differences can be found in Duvivier & Cassano (2015). The higher wind speeds are not unrealistic, and we have explained this in the text with the following: "Figure 5 also highlights that whilst the annual mean bias for wind speed is less than  $1.5 \text{ ms}^{-1}$  (Table 2), during certain periods, WRF simulates higher wind speeds than observed. However, these are not unrealistic values for this region, with a maximum observed wind speed of  $20.2 \text{ ms}^{-1}$  and a maximum simulated wind speed of  $22.3 \text{ ms}^{-1}$  for the KPCL location. The largest values and biases of wind speed occur during particularly strong katabatic events (northwesterly wind direction during winter). This was also found by Hines & Bromwich (2008) when using the same land surface scheme as in these simulations." (Line 298-302).*

Line 199: "WRF struggles to as accurately represent the wind direction" – Please see my answer above to Line 174. I could imagine that this is a common problem at places with very

steep and rugged topography along the Greenland coast, is it? How accurate is wind data measured at weather stations?

*We have now included this information in Table 1, and included a discussion of the errors in this section. It is a common problem in rugged and complex terrain areas, especially with very local scale wind patterns and abrupt changes in wind direction as seen in the northeast of Greenland. Changes can be seen in red in the manuscript. Please also see response to Line 174 which also covers this topic.*

Line 224: Any idea why WRF underestimates summer air temperatures?

*The mean bias in summer is largest at KPCL and is  $-1.8^{\circ}\text{C}$ . At KPCU, it is within the error estimate from the sensor manufacturer ( $\pm 0.2^{\circ}\text{C}$ ). The differences between the model output and observations are not statistically significant either. We have now included this in the text: “WRF slightly underestimates the air temperature during summer, however at KPCU, this is within the error estimate provided by the sensor manufacturer (Table 1), and for both locations the biases are not statistically significant (Table 2).” (Line 329-332)*

Line 236-239: On which time scales (how many days) do warm-air events occur? Can they really explain larger diurnal variability?

*The warm-air events are relatively frequent (10 times per year on average) and can last for approx. 2-4 days. If you look at Figure 2 in Turton et al 2019 (doi: 10.1175/MWR-D-18-0366.1) you can see the impact of a number of warm-air events in a single winter season. In combination with the larger variability in this season due to frequent storms and more variable weather conditions, they do have a clear impact on the winter variability.*

*We extended this section to make it clearer. It reads as: “However, the temperature variability is largest during winter over the glacier due to the more frequent passing of storms across the Atlantic Ocean and the occurrence of ‘warm-air events’ from easterly horizontal advection and increased longwave radiation from clouds (van As et al. 2009, Turton et al. 2019a). Warm-air events are characterised by large ( $>10^{\circ}\text{C}$ ) temperature increases between November and March, which can last for a number of days and, on average, occur 10 times per year (standard deviation of 4.0) (Turton et al. 2019a). The variability can be further enhanced by turbulent mixing from katabatic winds and the presence of föhn winds (Turton et al., 2019a).” (Line 347-353)*

#### Technical corrections:

Lines 56: Repetition of the word “fields” in one line. Please rephrase. Furthermore, I would rephrase the sentence to “Here we present an evaluation . . . to demonstrate the applicability . . .”

*Changed.*

Line 93: “floating tongue” – do you refer to the 79 North Glacier only? Otherwise it should be plural.

*In this sentence, we are referring only to the floating tongue of Spalte Glacier, not for 79N also, so it remains singular.*

Line 103: spacing between both sentences is missing

*Changed.*

Lines 102 – 112. This sentence is very long. I suggest to use bullet points for listing the different parameterizations.

*Thank you, we have split this into two sentences now. The use of the semi-colons for the list is preferable in our opinion.*

Lines 155-: I suggest to shift the Table 2 to a new page, i.e., there should be some text directly after the heading of section 3.1.

*Changed.*

Table 1: Please add °N/°W for units of the Location.

*Included.*

Figure 3: I suggest to use the same limits for the y-axis in a and b for easier comparison. (It would be easier to see that it gets colder at KPCU in winter.)

*Changed.*

Figure 4: Please give more details in the Figure captions. What do the percentages tell us? Why are maximum ranges of percentages different?

*We have now included that the percentages and circles relate to frequency of a particular wind direction. The maximum ranges are different as the occurrence of a particular wind direction can be very frequent (80% of the time wind was NNW for 24 August in WRF) or relatively infrequent (25 Aug 2014 in observations had variable wind with a maximum of 30% frequency for NNE wind). Although we attempted to have the same percentages shown for the left and right panels, it was difficult to read and interpret the data if 80% was used for all of them. For the 25<sup>th</sup> and 26<sup>th</sup> of August we were able to keep the same scale for observations and WRF output. But where they differed considerably, we used more appropriate scales. The caption now reads as: "Figure 5: Wind speed (colour) and direction (lines) for August 23 to 26 2014 from observations (left panel) and WRF (right panel) at KPCL location. The circles (and therefore length of the spikes) represent the frequency of the particular wind direction, with the percentage of occurrence written on the circles."*

## High-resolution (1 km) Polar WRF output for 79°N Glacier and the Northeast of Greenland from 2014-2018

Jenny V. Turton<sup>1</sup>, Thomas Mölg<sup>1</sup>, Emily Collier<sup>1</sup>

<sup>1</sup>Climate System Research Group, Institute of Geography, Friedrich-Alexander University, Erlangen-Nürnberg, 90158, Germany.

Correspondence to: Jenny V. Turton ([jenny.turton@fau.de](mailto:jenny.turton@fau.de))

### Abstract

The northeast region of Greenland is of growing interest due to changes taking place on the large marine-terminating glaciers which drain the north east Greenland ice stream.

Nioghalvfjerdingsfjorden, or 79°N Glacier, is one of these that is currently experiencing accelerated thinning, retreat and enhanced surface melt. Understanding both the influence of atmospheric processes on the glacier and **feedbacks from** changing surface **conditions** is crucial for our understanding of present stability and future change. However, relatively few studies have focused on the atmospheric processes in this region, and even fewer have used high-resolution modelling as a tool **to address** these research questions. Here we present a **high spatial- (1 km) and temporal- (up to hourly) resolution** atmospheric modelling dataset, NEGIS\_WRF, for the 79°N and northeast Greenland region from 2014-2018, and an evaluation of the model's success at representing daily near-surface meteorology **when** compared with automatic weather station records. The dataset, (Turton et al, 2019b: [doi.org/10.17605/OSF.IO/53E6Z](https://doi.org/10.17605/OSF.IO/53E6Z)), is now available for a wide variety of applications **in the** atmospheric, hydrological and oceanic **sciences in the study region**.

### 1. Introduction

The surface mass balance of a glacier is largely controlled by regional climate through varying mass gains and losses in the ablation and accumulation zones, respectively. The large amount of mass lost from the Greenland Ice Sheet (GrIS) within the last few decades (**approximately 3800 billion tonnes of ice between 1992 and 2018**; Shepherd et al., 2019) has largely been located around the coast of Greenland, due to the thinning and retreat of marine-terminating glaciers (Howat & Eddy, 2011), and the surface mass loss in the ablation zone **due to enhanced melting and runoff** (Rignot, et al., 2015; van den Broeke et al., 2017). **A recent study found that enhanced meltwater run off, connected to changing atmospheric conditions, was the largest contributor of mass loss for**

Greenland (52%) (Shepherd et al., 2019). The remaining 48% of mass loss (1.8 billion tonnes of ice) was due to enhanced glacier discharge, which has been increasing over time (Shepherd et al., 2019).

The majority of studies of the surface mass loss in Greenland and its atmospheric controls are largely constrained to southern and western Greenland (e.g Kuipers Munneke et al., 2018; Mernild et al., 2018), or to specific warm events such as the 2012 melt event (e.g Bennartz et al., 2013; Tedesco et al., 2013). However, recent studies have shown that the northeast of Greenland, specifically the North East Greenland Ice Stream (NEGIS) is now experiencing high ice velocity and accelerated thinning rates (Joughin et al., 2010; Khan et al., 2014). NEGIS extends into the interior of the Greenland ice stream by 600 km and three marine-terminating glaciers connect the NEGIS with the ocean. The largest of these glaciers is Nioghalvfjærdsfjorden, often named 79°N after its latitudinal position. Until recently, very few studies focused on 79°N glacier and NEGIS as they were thought to contribute little to surface mass loss and instabilities (Khan et al., 2014; Mayer et al., 2018). However, 79°N glacier, with its 80 km long by 20 km wide floating tongue, has retreated by 2-3 km between 2009 and 2012, and the surface of the tongue and part of the grounded section of the glacier are now thinning at a rate of  $1 \text{ m yr}^{-1}$  (Khan et al., 2014, Mayer et al. 2018). The glacier is at a crucial interface between a warming ocean and a changing atmosphere. The mass loss from the floating tongue is largely attributed to basal melting due to the presence of warm ( $1^{\circ}\text{C}$ ) ocean water in the cavity below the glacier (Wilson & Straneo, 2015, Schaffer et al., 2017, Münchow et al., 2019). However, even the grounded part of the glacier is characterised by large melt ponds and drainage systems (Hochreuther, P. pers. comm); suggesting that atmospheric processes may also be at play. Furthermore, atmospheric processes may be responsible for driving the warm Atlantic water under the glacier tongue, which leads to melting of the glacier base (Münchow et al., 2019). 79°N glacier is of further interest because its southerly neighbour, Zachariae Istrom, recently lost its floating tongue (Mouginot et al., 2015).

A number of studies have used atmospheric modelling as a tool to investigate the region, although they have largely been confined to short case studies (Turton et al., 2019a), focused on past climates (e.g 45000 years ago by Larsen et al., 2018), or targeted specific atmospheric processes (Leeson, et al., 2018; Turton et al., 2019a). There are a number of atmospheric models that have been applied to the Greenland region, however these are often run at a resolution that is too coarse to resolve the 79°N glacier, especially its floating tongue, which can therefore be missing in many simulations. These data are usually statistically downscaled to calculate the surface mass balance of the glacier, using a digital elevation model and a shape file of the glacier. The resolution of the atmospheric models used in published studies for Greenland generally exceed 10km: e.g the Modèle Atmosphérique Régional (MAR) at 20-km (Fettweis et al, 2017) RACMO2 at 11-km (Noël et

al., 2016) and HIRHAM5 at 25-km (Mottram et al., 2017a). Recently, there have been attempts at modelling the polar regions using non-hydrostatic regional climate models, including HARMONIE-AROME at 2 km resolution for the Southwest of Greenland (Mottram et al., 2017b), and the NHM-SMAP at 5 km resolution for the whole of Greenland (Niwano et al., 2018). However, the Mottram et al. (2017b) study does not include the northeast of Greenland. Furthermore, the focus of the Niwano et al. (2018) study was to improve the surface mass balance estimates, as opposed to providing output for a more general atmospheric sense, and the model was not convection permitting. As yet, there are no very high-resolution, multi-year atmospheric datasets available for the northeast of Greenland or the wider region.

Here, we address this data gap by presenting a 5-year (2014-2018), high-resolution (1 km) atmospheric simulation using a polar-optimised atmospheric model and evaluate its skill in representing local meteorological conditions over the 79°N region in northeast Greenland. The dataset is named NEGIS\_WRF after its location of focus and model used. As the 79°N region is of growing interest, this data could be beneficial for numerous other studies and applications. Indeed, current ongoing research as part of the Greenland Ice sheet-Ocean interaction (GROCE) project ([www.groce.de](http://www.groce.de), last accessed October 1 2019) include using this data for surface mass balance studies and to investigate the relationship between specific atmospheric processes and surface melt patterns. For studies of the surface mass balance of the NEGIS, further downscaling would not be necessary. With a horizontal resolution of less than 5km, many atmospheric processes are accurately resolved including katabatic winds and warm-air advection (Turton et al., 2019a). Furthermore, high-resolution output is crucial for the complex topography on the northeast coast, where steep and variable topography can channel or block the winds, and lead to strong variability of the radiation budget. The WRF dataset is also intended as input to an ocean model, used in an ocean-glacier interaction study, input into a hydrologic model and for an ice sheet modelling study. Here we present an evaluation of the ability of NEGIS\_WRF at representing key near-surface meteorological and radiative conditions, to demonstrate the applicability of the dataset for these and other studies in the atmospheric, cryospheric and oceanic fields.

## 2. Data and Methods

### 2.1 Model Configuration

The Polar Weather Research and Forecasting (Polar WRF) model is a version of the WRF model that was developed and optimised for use in polar climates (Hines et al., 2011). The non-hydrostatic WRF model (available online from <http://www.mmm.ucar.edu/weather-research-and-forecasting-model>; last accessed July 29 2019) has been widely used for both operational studies

and for research in many regions, and at many scales (Powers et al., 2017; Skamarock & Klemp, 2008). The current version of polar WRF used here is v3.9.1.1, which was released in January 2018, and is available from <http://polarmet.osu.edu/PWRF/> (last accessed July 29 2019). Polar WRF has been developed for use in the Arctic and Antarctic by largely optimising the Noah Land Surface Model (LSM) (Chen & Dudhia, 2001) to improve heat transfer processes through snow and permanent ice, and by providing additional methods for sea-ice treatment (Hines et al, 2015). For a full description of the Polar WRF additions, see (Hines & Bromwich, 2008; Hines et al., 2011; Hines et al., 2015) and citations therein.

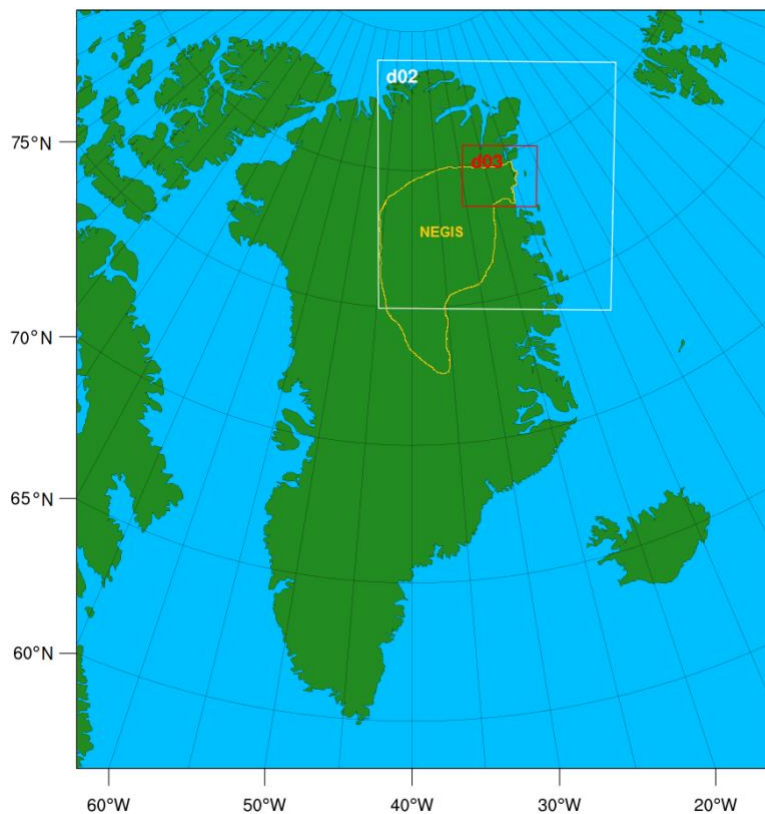


**Figure 1: The domain configuration for the Polar WRF runs and the approximate outline of NEGIS following Khan et al. (2014).**

The meteorological initialisation and boundary input data is from the ECMWF (European Centre for Medium range Weather Forecast) ERA-Interim dataset at 6-hourly intervals (Dee et al., 2011). This reanalysis product was more accurate at resolving mesoscale processes in the northeast of Greenland compared to MERRA2 reanalysis data and has previously been used for Polar WRF simulations in Greenland (DuVivier & Cassano, 2013; Turton et al., 2019a). The Sea Surface Temperature (SST) and sea ice concentration values are from the NOAA Optimum Interpolation 0.25° resolution daily data. This is a combination of data from the Advanced Very High Resolution

Radiometer (AVHRR) infrared satellite and Advanced Microwave Scanning Radiometer (AMSR) (doi:10.5065/EMOT-1D34, data retrieved from <https://rda.ucar.edu/datasets/ds277.7/>, last accessed July 29 2019). In-situ ship and buoy data are used to correct satellite biases, leading to relatively low mean biases of 0.2-0.4K for SST data (more information on this dataset can be found in Banzon et al., 2016). This higher resolution dataset was required due to the very blocky coastline in the SST and sea ice data from ERA-Interim. The domain setup is shown in Figure 1. The outermost domain (D01) is at 25km, D02 is 5km and D03 (innermost) is 1km grid spacing. Boundary conditions, including sea ice fraction and SST were updated every 6-hours. Analysis nudging was used in the outer domain (D01) to constrain the large-scale circulation while allowing the model to freely simulate in D02 and D03. Nudging is the process of constraining the interior of model domains towards the larger-scale field (from reanalysis data) which drive the simulation (Lo et al., 2008., Otte et al., 2012). It has been found to improve simulations of the large-scale circulation (Bowden et al., 2012) and reduce errors in the mean and extreme values (Otte et al., 2012) from relatively long runs. We only nudge the outer domain (D01) to allow the higher-resolution domain to evolve freely. The USGS 24 category landuse and landmask was adjusted using the European Space Agency (ESA) Climate Change Initiative (CCI) landuse product, to provide a better representation of the glacier outlines and the terminus of the floating tongue (<https://www.esa-landcover-cci.org/>, last accessed September 5 2019). A number of open-water grid points were manually changed to glacierised during January-June and September-December to better represent the floating tongue of the Spalte Glacier (tributary of 79°N on the northeast side) and the sea ice in the adjacent Dijnphna Sound (Fig. 2). Other small exposed water areas along the coast, which are permanently frozen except in July and August each year (Hochreuther, P., 2019 personal communication), were also changed to ice during all months except July and August (Fig. 2). The glacier extents are treated as static throughout the run, which is an appropriate approximation given the small and likely negligible area of calving of 79°N during our study period (see ENVEO, 2019 for calving front locations from 1990 to 2017). There are 60 levels in the vertical, with a 10-hPa model top and a lowest model level ~16m above the surface.

Many of the parameterisations for the model configuration were selected based on numerous, previous Polar WRF runs over Greenland and the Arctic (for example Hines et al., 2011). In brief, the following parameterisations were employed: the Noah LSM (Chen & Dudhia, 2011), due to its optimisations that have been tested over Greenland (Hines & Bromwich, 2008), Arctic sea ice (Hines, et al 2015) and Arctic land (Hines et al., 2011); the Morrison two-moment scheme for microphysics, which has been shown to out-perform other schemes in both Polar regions (Bromwich, et al., 2009; Lachlan-Cope, et al., 2016; Listowski & Lachlan-Cope, 2017); the Eta Similarity Scheme for surface layer physics (Janjić, 1994) and the Yonsei University Scheme for



planetary boundary layer parameterisation. This was used due to the topographic wind scheme (Hong et al., 2006) that can correct excessive wind speeds in areas of complex topography, such as the northeast coast of Greenland (employed in D02 and D03 only, where complex orography is best resolved). Further parameterisations include: the Kain-Fritsch scheme for cumulus convection (Kain, 2004) (D01 and D02 only, as the resolution of D03 allows convection to be explicitly resolved); and, the Rapid Radiative Transfer Model (RRTM) longwave and Goddard shortwave schemes for radiation, based on sensitivity testing for the polar regions by Hines et al. (2008) and subsequent runs over Greenland (DuVivier & Cassano, 2013; Hines et al., 2011). Whilst the majority of these options were selected for testing based on the works of other publications, a short sensitivity study was also conducted, alongside with testing the horizontal and vertical resolution and locations of the domains (not included). It was found that a combination of the options above were best suited to the northeast of Greenland when compared with observations on the floating tongue of the 79°N glacier from 1996-1999 (Turton et al., 2019a).

Other options specified for this study include using a fractional sea ice treatment, which allows calculation of different surface temperature, surface roughness and turbulent fluxes for open water and sea ice conditions within the grid cell, and then calculates an area-weighted average for the grid (DuVivier & Cassano, 2013; Hines et al., 2011). The adaptive timestep was used to optimise the simulation speed. For each year simulated, the model was initialised on September 1 before the onset of the accumulation season and ran continuously until October 1 of the following year (e.g September 1 2016 - October 1 2017). September was then discarded as a spin up month. The model produces similar magnitude snow depths to available observations (Pedersen et al. 2016). Due to limited snowfall and snow depth observations in this region, we compared cumulative snowfall to ERA5 products during testing, which have been shown to have a relatively good agreement with observations by Wang et al. (2019). The maximum snow depth and average annual accumulation were well captured by Polar WRF compared to ERA5.

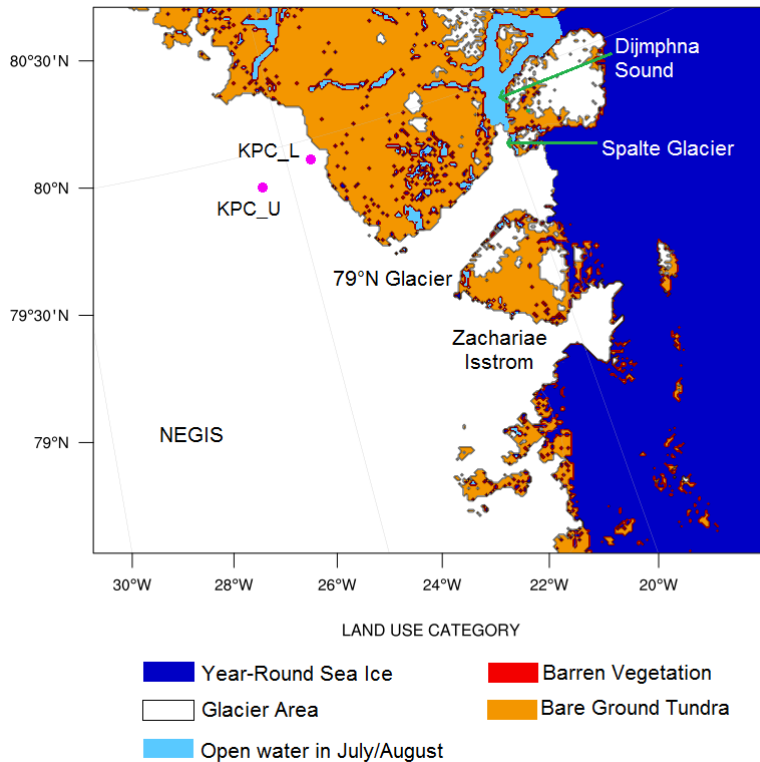


**Figure 2: A map of the land use types for D03. Colours represent the land use type, except for light blue, which highlights the manually changed land use from open water to sea ice during winter. Important locations are also highlighted, as are the locations of the two AWS sites (pink dots).**

The data were output at hourly intervals for D03, at six-hourly intervals for D02 and at daily intervals for D01. Daily mean values for key meteorological variables from D02 and D03 were calculated from the hourly values and are available along with the daily instantaneous values from D01 at the Open Science Framework repository (Turton et al. 2019b: [doi.org/10.17605/OSF.IO/53E6Z](https://doi.org/10.17605/OSF.IO/53E6Z)).

## 2.2 Observational Data

The remote nature of the location of interest provides few in-situ observational datasets for model evaluation. However, the PROMICE (Programme for Monitoring of the Greenland Ice Sheet) network ([www.promice.dk](http://www.promice.dk), last accessed October 1 2019; van As & Fausto, 2011), operated by the Geological Survey of Denmark and Greenland (GEUS) has two permanent Automatic Weather Stations (AWSs) available for comparison of daily means of meteorological variables and a number of surface energy balance components. The AWSs are referred to as KPC\_L and KPC\_U due to their location on Kronprins Christian Land (located to the northwest of 79°N glacier; see Table 1 for AWS details of location, dates and available variables. Although hourly data are available, daily means are used for evaluation due to the multi-year timescale of the study, but the authors note that an evaluation of

hourly data should be performed before using these data for analysis at these time scales. Please refer to van As & Fausto, (2011) and Turton et al., (2019a) for more information on the PROMICE data in this location (doi.org/10.22008/promice/data/aws, available at [www.promice.dk](http://www.promice.dk), last accessed October 1 2019). **Observations are not taken at exactly 2m above the surface but vary with accumulation and ablation. Over bare ice, the sensor is 2.6m above the surface (van As et al., 2011). To clarify that the observations represent near-surface conditions, and are compared with 2m and 10m model output, we use the abbreviation X2 or X10 to represent both modelled and observed variables at the respective heights.** The mean values from the observational data are calculated from daily averages from January 1 2014- December 31 2018 to keep a consistent period across all data.

The in-situ AWS observational data are used to evaluate the NEGIS\_WRF output and to provide a judgement of its skill to benefit future users. The focus of the evaluation is to test WRF's ability to represent local meteorological conditions over a polar glacier. Daily mean values from NEGIS\_WRF have been calculated from hourly output at the location of the two AWSs. All evaluation focuses on near-surface meteorological output from D03.

**Table 1: The location, elevation and data availability of the two AWSs used for model evaluation. We evaluate the model output with four variables from the AWSs. Data was unavailable at KPC\_L between January 15 2010 and July 17 2012 due to retrieval problems. T is air temperature, Q is specific humidity, WS and WD are wind speed and direction, respectively. **Observations are taken at approximately 2m above the surface, but this does vary with accumulation and ablation (see section 2.2). Sensor error estimates come from the sensor manufacturers. See van As & Fausto (2011) for more information on sensors and observations.****

Name	Location	Elevation (m a.s.l)	Data Availability	Variables used for evaluation	Sensor Error Estimates
KPC_L	79.91°N, 24.08°W	380	01.01.2009- present	T, Q, WS, WD, SW <sub>down</sub> , LW <sub>down</sub>	T: ± 0.2°C RH: ± 1.5% WS: ± 0.3ms <sup>-1</sup> WD: ± 3° Radiation: 10%
KPC_U	79.83°N, 25.17°W	870	01.01.2009- 14.01.2010,	T, Q, WS, WD, SW <sub>down</sub> , LW <sub>down</sub>	T: ± 0.2°C RH: ± 1.5% WS: ± 0.3ms <sup>-1</sup> WD: ± 3°

			18.07.2012-present		Radiation: 10%
--	--	--	--------------------	--	----------------

### 3. Results

#### 3.1 Model evaluation: Daily Means

The air temperature is simulated well by the WRF simulations with a **coefficient of determination ( $R^2$ ) of 0.92** at both KPC\_L and KPC\_U (Table 2, Fig 3). Similarly, the mean biases and RMSE are small. The mean bias and RMSE are slightly larger during winter (DJF) at KPC\_U, but overall, the  **$R^2$  value** at both locations remains above **0.64**. The particularly low daily temperatures observed during winter at KPC\_U are not fully captured by the WRF simulations (Fig. 3b). The model can, however, capture the larger variability in winter (Fig. 3), including ‘warm-air events’, where the air temperature increases by more than 10°C in a few days, leading to temperatures above the average for winter (Turton et al., 2019a). **Figure 4 presents the near-surface air temperature and 10m wind vectors for June 6 2015, to show what the temperature and wind fields look like for an example time period during the ablation period (June to August). The onset of the ablation season is earlier over the floating tongue of the glacier, as seen by the above freezing air temperatures at low elevations in Figure 4.** WRF simulates the humidity very well annually and during winter for both locations. The humidity during summer is slightly less well simulated, with mean biases of 0.4 and 0.6 g/kg for KPC\_L and KPC\_U respectively (Table 2). However, **the  $R^2$  values remain above 0.44** for the summer season. For both locations, annually and seasonally, WRF is moister than in observations, however the mean biases remain relatively small (less than 0.6 g/kg), and the differences are not statistically significant except for during summer at KPC\_U (which is statistically different at the 99% confidence level using a student t-test). The wind direction in WRF **deviates more from the AWS data** than for temperature and moisture, **which is likely due to the particularly steep and complex topography of the region which may not be accurately represented by the model, even at 1 km resolution.** The largest bias is an annual bias at KPC\_L (10.7°) as WRF simulates the wind direction predominantly more northerly than in observations (Table 2), which leads to poor  **$R^2$  values (0.01)** and high RMSE. For KPC\_U annually and seasonally, the biases remain at or below 8.6° and  **$R^2$  values are 0.36**, which shows that WRF is capable of representing the wind direction at KPC\_U. **Some of these errors may relate to measurement errors of the wind sensor, which is  $\pm 3^\circ$  (see Table 1).** The model performs **better at simulating the wind speed than the wind direction.** Annually and during winter, the  **$R^2$  values** are relatively high (above **0.31**) at both locations, and mean biases remain at or below 2.3 ms<sup>-1</sup>

<sup>1</sup> both annually and seasonally. None of the biases between WRF and observations are statistically significantly different for daily mean wind speed or air temperature (Table 2).

Shortwave and longwave radiation values are important for a range of possible future studies including input to surface mass balance and ocean models. Therefore, we have validated the NEGIS\_WRF output for both the downwelling shortwave and longwave by comparing it to observations at the two sites (Table 2). Annually, the biases are within sensor error range (Table 1) and differences between WRF and observations are not statistically significant for both downwelling shortwave ( $SW_{down}$ ) and longwave ( $LW_{down}$ ). Due to the lack of sunlight during winter at this latitude, the  $SW_{down}$  biases and RMSE are small and the  $R^2$  values (0.78 and 0.75 for KPC\_L and KPC\_U respectively) are high for both locations (Table 2). The mean biases are largest for  $SW_{down}$  during summer, but a relatively high  $R^2$  value shows that WRF still has a great deal of skill (0.82 at KPC\_U). Biases for  $LW_{down}$  are largest during winter (-10.3 and -15.3  $Wm^{-2}$  at KPC\_L and KPC\_U respectively), which is likely a product of increased wintertime variability due to storm frequency and location (van As et al., 2009). Similarly, Cho et al. (2020) found that biases of  $LW_{down}$  compared to satellite observations were larger for the Morrison microphysics scheme (which we use here) than for another scheme. However, it was concluded that Polar WRF has the ability to accurately simulate the spatial distribution of Arctic clouds and their optical properties with both schemes (Cho et al., 2020). None of the differences between WRF output and observations for the radiation components were statistically significant (Table 2).

**Table 2: Comparison of the near-surface WRF model output to AWS data at KPC\_L and KPC\_U. ANN refers to annual mean values, DJF refers to winter average values whereas JJA refers to summer average values. \* refers to statistically significant differences between WRF and AWS at the 99% confidence interval, using the student's t-test.**

Variable (units)	Location	AWS Mean	Mean Bias (WRF-AWS)	RMSE	$R^2$
T2 ANN (°C)	KPC_L	-13.6	-0.3	3.0	<b>0.92</b>
	KPC_U	-17.2	1.8	4.0	<b>0.92</b>
T2 DJF (°C)	KPC_L	-23.3	0.0	3.2	<b>0.86</b>
	KPC_U	-27.6	2.6	5.2	<b>0.64</b>
T2 JJA (°C)	KPC_L	1.6	-1.8	2.6	<b>0.71</b>
	KPC_U	-1.5	-0.1	1.9	<b>0.69</b>
Q2 ANN (g/kg)	KPC_L	1.6	0.2	0.4	<b>0.92</b>
	KPC_U	1.4	0.3	0.5	<b>0.92</b>

Q2 DJF (g/kg)	KPC_L	0.4	0.1	0.1	0.81
	KPC_U	0.3	0.1	0.2	0.66
Q2 JJA (g/kg)	KPC_L	3.2	0.4	0.8	0.44
	KPC_U	3.0	0.6*	0.9	0.56
WD10 ANN (°)	KPC_L	219.4	10.7*	74.3	0.01
	KPC_U	277.9	3.4	29.9	0.36
WD10 DJF (°)	KPC_L	238.5	-3.2	49.9	0.01
	KPC_U	274	8.6	29.1	0.36
WD10 JJA (°)	KPC_L	211.6	6.8*	80.2	0.01
	KPC_U	279.9	-0.1	31.7	0.25
WS10 ANN (m/s)	KPC_L	5.7	0.4	2.9	0.42
	KPC'_U	4.8	1.5	2.5	0.49
WS10 DJF (m/s)	KPC_L	6.4	1.0	3.2	0.50
	KPC_U	5.2	2.3	3.4	0.38
WS10 JJA (m/s)	KPC_L	5.4	-0.8	2.7	0.31
	KPC_U	4.2	0.8	1.9	0.45
SW <sub>down</sub> ANN (Wm <sup>-2</sup> )	KPC_L	114.5	4.7	34.1	0.94
	KPC_U	124.6	3.8	23.8	0.97
SW <sub>down</sub> DJF (Wm <sup>-2</sup> )	KPC_L	0.1	-0.1	0.4	0.78
	KPC_U	0.2	-0.1	0.5	0.75
SW <sub>down</sub> JJA (Wm <sup>-2</sup> )	KPC_L	271.6	13.1	62.3	0.63
	KPC_U	295.1	11.9	42.2	0.82
LW <sub>down</sub> ANN (Wm <sup>-2</sup> )	KPC_L	212.0	-7.1	24.7	0.76
	KPC_U	202.5	-9.2	26.1	0.71
LW <sub>down</sub> DJF (Wm <sup>-2</sup> )	KPC_L	181.9	-10.3	26.8	0.50
	KPC_U	179.6	-15.3	31.6	0.40
LW <sub>down</sub> JJA (Wm <sup>-2</sup> )	KPC_L	267.3	-4.9	23.8	0.38
	KPC_U	250.8	-6.4	21.6	0.49

The larger RMSE and lower  $R^2$  values during summer for wind direction can, at least partly, be attributed to the larger variability of those variables during summer. In summer (JJA), the average deviation of wind direction in observations at KPC\_L is 40.3°. Whilst WRF is able to capture this variability in wind direction (the average deviation is 41.1°), there is sometimes an offset in the timing of the wind direction change between WRF and observations. For example, after two weeks of consistently northwesterly winds being observed at KPC\_L between August 11 to 24, 2014, there was

a shift to northeasterly flow on the morning of August 25 2014 (Fig 5e). WRF successfully simulated the long period of northwesterly winds, and the shift to winds from the northeast, however the change in direction was simulated in the late evening of August 25 to early morning of August 26 (Fig. 5f), leading to a bias of  $156.9^\circ$  on August 25. The northeasterly wind was only observed for 24 hours before returning to westerly on August 26 (Fig. 5g). WRF was able to capture the short-lived timing of the event, but 24 hours later. In this particular case, the wind direction error comes from the boundary data, ERA-Interim. In ERA-Interim, the wind direction change starts on August 24 but remains northerly until 18:00 UTC on August 25. It then remains northeasterly until August 27, which is 24-hours longer than in near-surface observations. The later onset and more persistent flow from the northeast in ERA-Interim likely led to the later onset of northeasterly flow in WRF. Therefore, WRF can capture both the predominant wind flow, and abrupt changes to the wind direction, along with capturing even short-lived events, although the timing is occasionally shifted. Figure 5 also highlights that whilst the annual mean bias for wind speed is less than  $1.5 \text{ ms}^{-1}$  (Table 2), during certain periods, WRF simulates higher wind speeds than observed. However, these are not unrealistic values for this region, with a maximum observed wind speed of  $20.2 \text{ ms}^{-1}$  and a maximum simulated wind speed of  $22.3 \text{ ms}^{-1}$  for the KPCL location. The largest values and biases of wind speed occur during particularly strong katabatic events (northwesterly wind direction during winter). This was also found by Hines & Bromwich (2008) when using the same land surface scheme as in these simulations.

Overall, WRF performs well at simulating air temperature, humidity, downwelling radiation and wind speed during the simulation period (Oct 2013 - Dec 2018). WRF struggles to as accurately represent the wind direction, especially at KPC\_L (which is likely due to the proximity of complex topography to the KPC\_L site), however the winds remain predominantly westerly to northwesterly, which shows that WRF can capture the dominant katabatic process governing the wind directions.

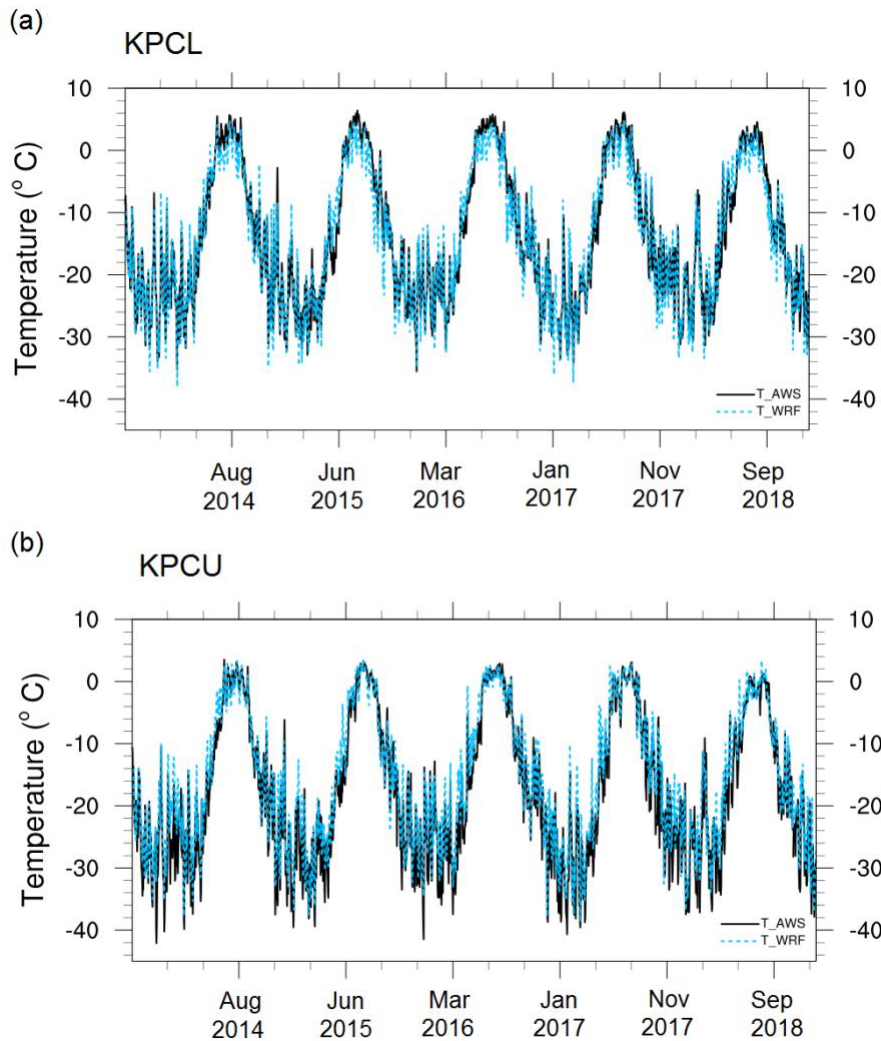


**Figure 3: The observed (black lines) and modelled (dashed blue lines) daily average air temperature at KPC\_L (top) and KPC\_U (bottom) from D03.**

### 3.2 Model evaluation: Sub-daily Data

To evaluate the ability of the model to simulate sub-daily values, the minimum and maximum daily near-surface values (from hourly output) are compared to observations, and the amplitude of the diurnal cycle of air temperature is also evaluated. Figure 6 presents the statistics for daily minimum and maximum air temperatures at the two locations in observations and WRF. The median values are well captured by WRF, especially for the maximum daily values, where a median value of  $-13.9^{\circ}\text{C}$  is observed at KPC\_U, and  $-14.0^{\circ}\text{C}$  is simulated. Similarly, for maximum temperatures, the 75<sup>th</sup> quartile values are well captured by WRF (Fig. 6). For KPC\_L, the minimum and maximum temperatures are colder in WRF than in observations. For example, the 25<sup>th</sup> percentile value for the minimum temperatures (far left bar in Fig. 6) is  $3.8^{\circ}\text{C}$  in observations, but  $6.3^{\circ}\text{C}$  in WRF. At KPC\_U, the opposite is true, where WRF simulates slightly higher temperatures than in observations.



However, overall, the range of minimum and maximum temperature values are well modelled by WRF.

The average daily maximum air temperature observed at KPC\_L is  $-21.0^{\circ}\text{C}$  in winter (DJF) and increases to  $3.0^{\circ}\text{C}$  in summer (JJA). WRF simulates an average daily maximum of  $-20.9^{\circ}\text{C}$  in winter, which increases to  $0.9^{\circ}\text{C}$  in summer. The average daily minimum air temperature observed at KPC\_L is  $-25.9^{\circ}\text{C}$  during winter and rises to  $0.2^{\circ}\text{C}$  in summer. WRF simulates an average daily minimum air temperature of  $-26.5^{\circ}\text{C}$  in winter and increasing to  $-2.3^{\circ}\text{C}$  in summer. Therefore, WRF is able to accurately simulate the winter minimum and maximum temperatures. WRF slightly underestimates the air temperature during summer, however at KPC\_U, this is within the error estimate provided by the sensor manufacturer (Table 1), and for both locations the biases are not statistically significant (Table 2).

Similarly, at KPC\_U, the observed maximum temperature values are  $-24.1^{\circ}\text{C}$  in winter and  $0.1^{\circ}\text{C}$  in summer. From WRF, the average maximum temperature is  $-22.5^{\circ}\text{C}$  in winter and increases to  $-0.1^{\circ}\text{C}$  in summer. The observed minimum daily air temperature at KPC\_U is  $-30.8^{\circ}\text{C}$  during winter and  $-3.5^{\circ}\text{C}$  in summer. In comparison, in the WRF simulations, the average daily minimum temperature is  $-27.4^{\circ}\text{C}$  during winter and increases to  $-3.9^{\circ}\text{C}$  in summer. WRF can therefore represent the maximum and minimum daily air temperatures at KPC\_U.

The annual-average observed diurnal air temperature amplitude is  $5.6^{\circ}\text{C}$  at KPC\_U and  $4.0^{\circ}\text{C}$  at KPC\_L. The largest average diurnal cycle is observed during spring (MAM) at KPC\_U ( $6.8^{\circ}\text{C}$ ) and during winter at KPC\_L ( $4.9^{\circ}\text{C}$ ). The WRF model simulated an average diurnal amplitude of  $5.0^{\circ}\text{C}$  at KPC\_U  $4.7^{\circ}\text{C}$  at KPC\_L. The largest diurnal cycles are simulated during spring at KPC\_U ( $6.2^{\circ}\text{C}$ ) and during winter at KPC\_L ( $5.5^{\circ}\text{C}$ ). Therefore, WRF accurately simulates the timing of the largest diurnal amplitudes but overestimates the amplitude slightly at KPC\_L, and underestimates it at KPC\_U, both by  $0.6^{\circ}\text{C}$ . The relatively large diurnal amplitude in winter may be counterintuitive given that the glacier is located in the Arctic, where polar night (no solar radiation) prevails throughout winter. However, the temperature variability is largest during winter over the glacier due to the more frequent passing of storms across the Atlantic Ocean and the occurrence of 'warm-air events' from easterly horizontal advection and increased longwave radiation from clouds (van As et al. 2009, Turton et al. 2019a). Warm-air events are characterised by large ( $>10^{\circ}\text{C}$ ) temperature increases between November and March, which can last for a number of days and, on average, occur 10 times per year (standard deviation of 4.0) (Turton et al., 2019a). The variability can be further enhanced by turbulent mixing from katabatic winds and the presence of föhn winds (Turton et al., 2019a).

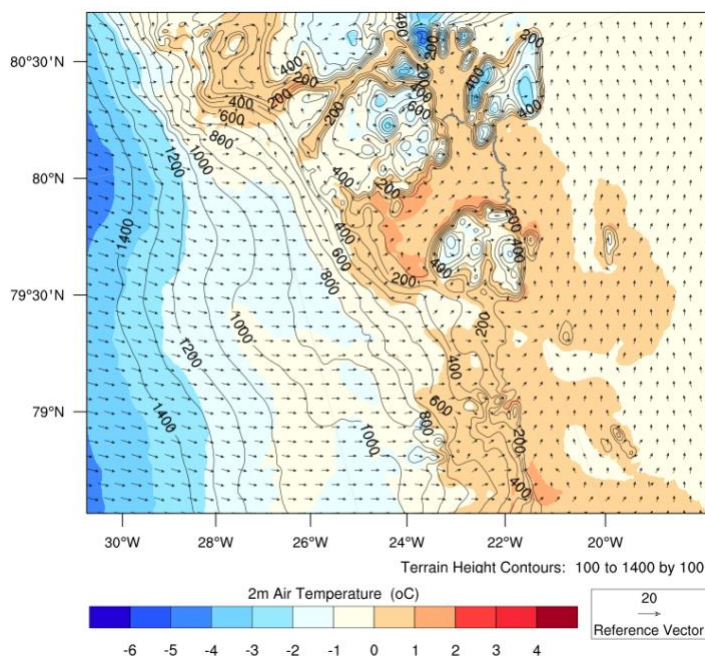


**Figure 4: The 2m air temperature (colours), wind vectors (arrows) and terrain height contours (black lines) for June 6 2015. The edge of 79°N glacier is shown by the dark grey line.**

The maximum hourly air temperature over the four years of data observed at KPC\_L was on July 23, 2014 (8.1°C) (Fig. 6). WRF was able to replicate the processes responsible for the particularly warm day, as a daily maximum value of 4.5°C was modelled at KPC\_U. At KPC\_L, the maximum was simulated 24-hours earlier (6.5°C). The maximum values from WRF are slightly lower than observed (Fig. 6), but the timing of the maximum was accurate. The lower maximum values are likely linked to the negative mean bias in temperature simulated by WRF during the summer months (Table 2).

The absolute minimum hourly air temperature was observed at KPC\_U on December 26, 2015 (-45.0°C) (Fig. 6) and on December 27, 2015 at KPCL (-37.2°C). Again, WRF was able to capture the events leading to the particularly cold December 2015 period. On December 27, the simulated minimum air temperature was -37.7°C at KPC\_L and -37.8°C at KPC\_U. The minimum daily values are warmer than those observed at KPC\_U, but very similar to those observed at KPC\_L. (Table2).

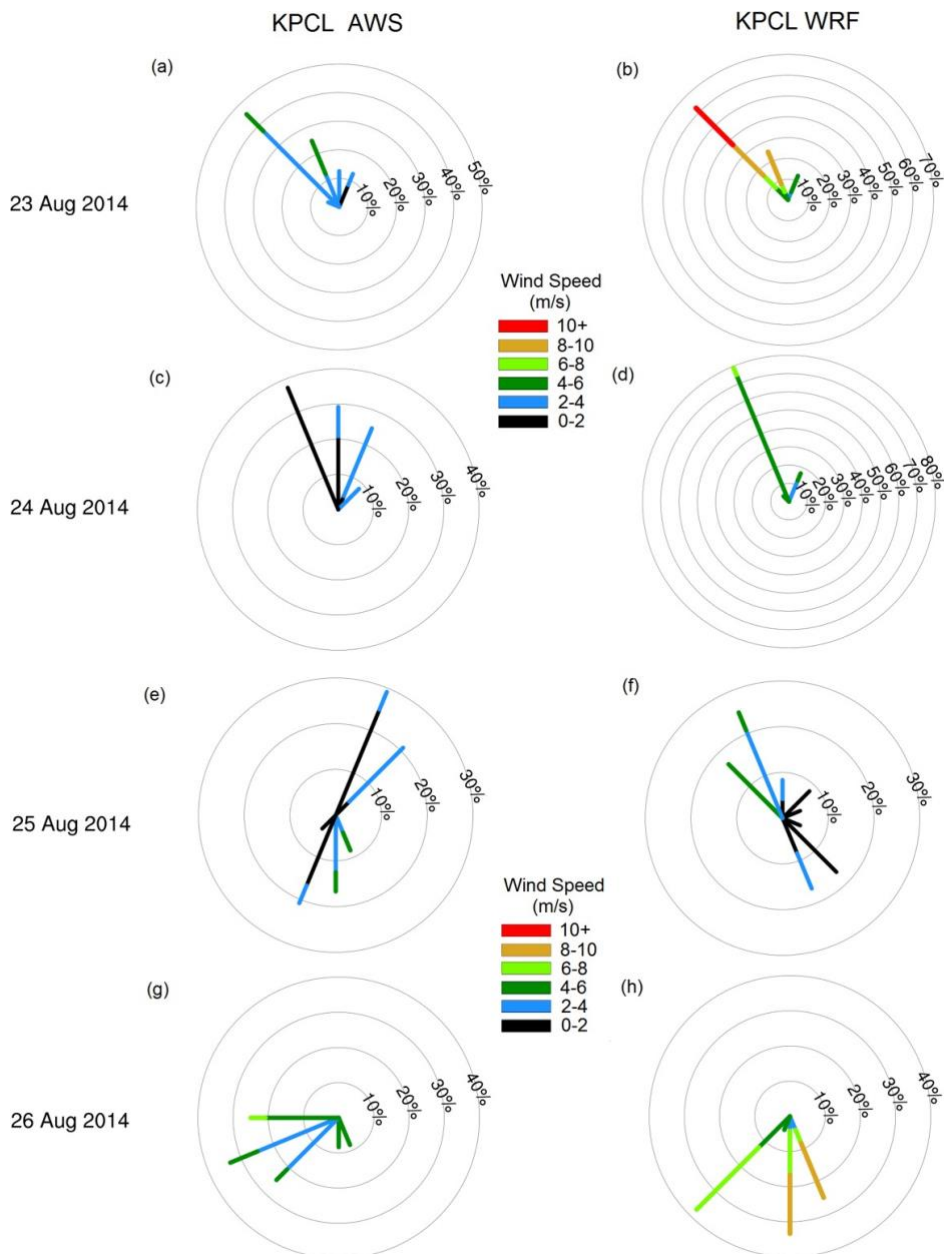


**Figure 5: Wind speed (colour) and direction (lines) for August 23 to 26, 2014, from observations (left panel) and WRF (right panel) at KPC\_L location. The circles (and therefore length of the spikes) represent the frequency of the particular wind direction, with the percentage of occurrence written on the circles.**

#### 4. Conclusions

Polar WRF has previously been extensively used in the Arctic (e.g Hines et al., 2011; Hines, & Bromwich, 2017; Wilson et al., 2011), including for Greenland (e.g DuVivier & Cassano., 2013; Turton et al., 2019a), for a number of applications. However, WRF runs have often been used for short case studies or performed at lower spatial resolution. This dataset provides high spatial and temporal resolution runs over multiple years (2014-2018) for an area of increased interest. Regardless of the

regular use of Polar WRF, it remains important to validate the model for specific locations, especially when downscaling to very high resolutions.

Overall, the mean biases are small and statistically insignificant between the Polar WRF runs and the PROMICE observations at both the lower and upper stations near 79°N glacier. The  $R^2$  values are high for air temperature, humidity and wind speed, but less so for wind direction at KPC\_L. The wind direction is more variable in summer than in other months, and whilst WRF is able to simulate the increased variability, large biases can arise due to inconsistent timing of wind direction changes between WRF and observations over short periods of 24-hours or less. However, as WRF is able to replicate the short-lived events and the predominant northwesterly winds of katabatic origin, we can conclude that the NEGIS\_WRF can be used for further studies of the near-surface meteorology of the 79°N glacier. This dataset will be useful for many other applications in a number of fields including the atmospheric and cryospheric sciences, and as input to hydrological, ice sheet and ocean models, **subject to appropriate validation**.

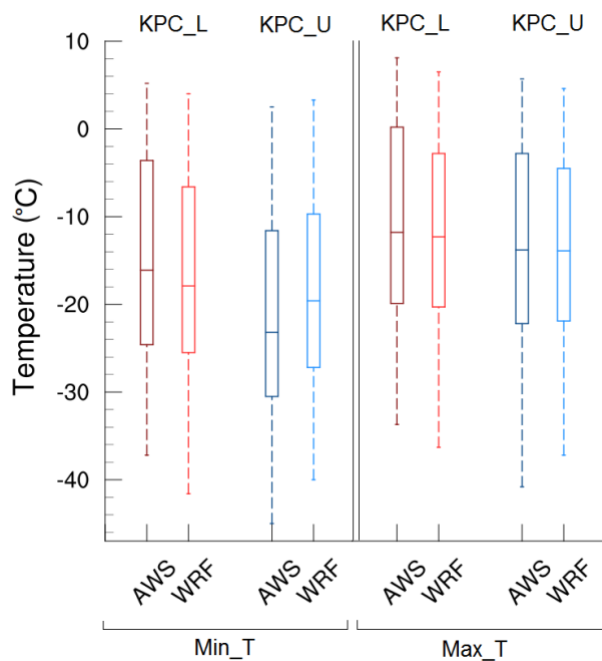


**Figure 6: Box plot representing the minimum (left) and maximum (right) daily temperature values at KPC\_L (red) and KPC\_U (blue) locations, from both observations (darker colours) and WRF (lighter colours).**

## 5. Data Availability

The atmospheric dataset, NEGIS\_WRF resolves for the first time, the meteorological conditions over the northeast region of Greenland (5km) and 79°N glacier region at the kilometre scale over a period

of five years (2014–2018). More than 50 variables are available (near-surface and on 60 atmospheric levels) at up to hourly temporal resolution (for the 1 km domain), including meteorological and radiative fields. Daily mean values for near-surface temperature (2m), specific humidity (2m), skin temperature, and U and V wind components (10m) are available online (Turton et al 2019b: [doi.org/10.17605/OSF.IO/53E6Z](https://doi.org/10.17605/OSF.IO/53E6Z)) for the 1km and 5km domains from 2014–2018. As the output frequency from D01 (25km resolution) was once per day, the available values are instantaneous daily values at 00 UTC, as opposed to daily means. Furthermore, 4-D variables of temperature, humidity, U and V wind components, geopotential and pressure are available on model levels at the same frequency as the near-surface variables. For other variables, or more frequent output, please contact the lead author, and these can be made available. Due to the large amount of data, these are not stored online, but at the Regional Computation Centre Erlangen (RRZE) in Germany.

## 6. Author Contributions

JVT wrote the paper, ran the WRF model and evaluated it against the observations. TM and EC contributed to the research concept, discussion, optimisation of the simulations and manuscript refinement.

## 7. Competing Interests

The authors have no competing interests.

## 8. Acknowledgements

We thank Dirk van As from GEUS for his assistance with the PROMICE data and to Keith Hines for the Polar WRF code. **The authors also thank two anonymous reviewers and Dr Yasuhiro Murayama for improving and editing our manuscript.** This work was supported by the German Federal Ministry for Education and Research (BMBF) and forms part of the GROCE project (Greenland Ice Sheet/Ocean Interaction) (Grant O3F0778F). We acknowledge the High Performance Computing Centre (HPC) at the University of Erlangen-Nürnberg's Regional Computation Centre (RRZE), for their support and resources whilst running the Polar WRF simulations.

## 9. References

**Banzon, V., Smith, T.M., Chin, T.M., Liu, C. & Hankins, W. (2016). A long-term record of blended satellite and in situ sea-surface temperature for climate monitoring, modelling and environmental studies. *Earth Syst. Sci. Data*, 8, 165–176. <https://doi.org/10.5194/essd-8-165/2016>**

- Bennartz, R., Shupe, M. D., Turner, D. D., Walden, V. P., Steffen, K., Cox, C. J., ... Pettersen, C. (2013). July 2012 Greenland melt extent enhanced by low-level liquid clouds. *Nature*, 496(7443), 83–86. <https://doi.org/10.1038/nature12002>
- Bowden, J.H., Nolte, C.G. & Otte, T.L. (2013). Simulating the impact of the large-scale circulation on the 2-m temperature and precipitation climatology. *Clim. Dyn.*, 40, 1903-1920. <https://doi.org/10.1007/s00382-012-1440-y>
- Bromwich, D. H., Hines, K. M., & Bai, L. (2009). Development and testing of Polar Weather Research and Forecasting model: 2. Arctic Ocean. *Journal of Geophysical Research*, 114(D8), D08122. <https://doi.org/10.1029/2008JD010300>
- Chen, F & Dudhia, J. (2001). Coupling an advanced land surface-hydrology model with the Penn State-NCAR MM5 modeling system. Part 1: Model implementation and sensitivity. *Monthly Weather Review*. 129, 569-585. [https://doi.org/10.1175/15200493\(2001\)129<0569:CAALSH>2.0.CO;2](https://doi.org/10.1175/15200493(2001)129<0569:CAALSH>2.0.CO;2)
- Cho, H., Jun, S-Y., Ho, C-H. & McFarquhar, G. (2020). Simulations of winter Arctic clouds and associated radiation fluxes using different cloud microphysics schemes in the Polar WRF: Comparisons with CloudSat, CALIPSO and CERES. *JGR:Atmospheres*, Accepted. <https://doi.org/10.1029/2019JD031413>
- Dee, D. P., Uppala, S. M., Simmons, A. J., Berrisford, P., Poli, P., Kobayashi, S., ... Vitart, F. (2011). The ERA-Interim reanalysis: configuration and performance of the data assimilation system. *Quarterly Journal of the Royal Meteorological Society*, 137(656), 553–597. <https://doi.org/10.1002/qj.828>
- DuVivier, A. K., & Cassano, J. J. (2013). Evaluation of WRF Model Resolution on Simulated Mesoscale Winds and Surface Fluxes near Greenland. *Monthly Weather Review*, 141(3), 941–963. <https://doi.org/10.1175/MWR-D-12-00091.1>
- ENVEO (2019), Greenland Calving Front Dataset, 1990-2017, v3.0, Greenland Ice Sheet CCI, from <http://cryoportals.enveo.at>
- European Space Agency Climate Change Initiative landuse product, available from <https://www.esalandcover-cci.org/>, last accessed September 5 2019.
- Fausto, R.S and van As, D. (2019). Programme for monitoring of the Greenland ice sheet (PROMICE): Automatic weather station data. Version: v03, Dataset published via Geological Survey of Denmark and Greenland. <https://doi.org/10.22008/promice/data/aws>
- Fettweis, X., Box, J. E., Agosta, C., Amory, C., Kittel, C., Lang, C., ... Gallée, H. (2017). Reconstructions of the 1900-2015 Greenland ice sheet surface mass balance using the regional climate MAR model. *The Cryosphere*, 11(2), 1015–1033. <https://doi.org/10.5194/tc-11-1015-2017>
- Hines, K. M., & Bromwich, D. H. (2008). Development and Testing of Polar Weather Research and

- Forecasting (WRF) Model. Part I: Greenland Ice Sheet Meteorology\*. *Monthly Weather Review*, 136(6), 1971–1989. <https://doi.org/10.1175/2007MWR2112.1>
- Hines, K. M., Bromwich, D. H., Bai, L.-S., Barlage, M., Slater, A. G., Hines, K. M., ... Slater, A. G. (2011). Development and Testing of Polar WRF. Part III: Arctic Land\*. *Journal of Climate*, 24(1), 26–48. <https://doi.org/10.1175/2010JCLI3460.1>
- Hines, K. M., Bromwich, D. H., Bai, L., Bitz, C. M., Powers, J. G., Manning, K. W., ... Manning, K. W. (2015). Sea Ice Enhancements to Polar WRF\*. *Monthly Weather Review*, 143(6), 2363–2385. <https://doi.org/10.1175/MWR-D-14-00344.1>
- Hines, K. M., & Bromwich, D. H. (2017). Simulation of Late Summer Arctic Clouds during ASCOS with Polar WRF. *Monthly Weather Review*, 145(2), 521–541. <https://doi.org/10.1175/MWR-D-16-0079.1>
- Hochreuther, P, Friedrich Alexander Universtiy, Personal Communication, July 2019
- Hong, S.-Y., Noh, Y., Dudhia, J., Hong, S.-Y., Noh, Y., & Dudhia, J. (2006). A New Vertical Diffusion Package with an Explicit Treatment of Entrainment Processes. *Monthly Weather Review*, 134(9), 2318–2341. <https://doi.org/10.1175/MWR3199.1>
- Howat, I. & Eddy, A. (2011). Multi-decadal retreat of Greenland's marine-terminating glaciers. *Journal of Glaciology*, 57(203), 389-396. Doi:10.3189/002214311796905631
- Janjić, Z. I. (1994). The Step-Mountain Eta Coordinate Model: Further Developments of the Convection, Viscous Sublayer, and Turbulence Closure Schemes. *Monthly Weather Review*, 122(5), 927–945. [https://doi.org/10.1175/15200493\(1994\)122<0927:TSMECM>2.0.CO;2](https://doi.org/10.1175/15200493(1994)122<0927:TSMECM>2.0.CO;2)
- Joughin, I., Smith, B. E., Howat, I. M., Scambos, T., & Moon, T. (2010). Greenland flow variability from ice-sheet-wide velocity mapping. *Journal of Glaciology*, 56(197), 415–430. <https://doi.org/10.3189/002214310792447734>.
- Kain, J. S. (2004). The Kain–Fritsch Convective Parameterization: An Update. *Journal of Applied Meteorology*, 43(1), 170–181. [https://doi.org/10.1175/1520-0450\(2004\)043<0170:TKCPAU>2.0.CO;2](https://doi.org/10.1175/1520-0450(2004)043<0170:TKCPAU>2.0.CO;2)
- Khan, S. A., Kjær, K. H., Bevis, M., Bamber, J. L., Wahr, J., Kjeldsen, K. K., ... Muresan, I. S. (2014). Sustained mass loss of the northeast Greenland ice sheet triggered by regional warming. *Nature Climate Change*, 4(4), 292–299. <https://doi.org/10.1038/nclimate2161>
- Kuipers Munneke, P., Smeets, C. J. P. P., Reijmer, C. H., Oerlemans, J., van de Wal, R. S. W., & van den Broeke, M. R. (2018). The K-transect on the western Greenland Ice Sheet: Surface energy balance (2003–2016). *Arctic, Antarctic, and Alpine Research*, 50(1), e1420952. <https://doi.org/10.1080/15230430.2017.1420952>
- Lachlan-Cope, T., Listowski, C., & O'Shea, S. (2016). The microphysics of clouds over the

- Antarctic Peninsula - Part 1: Observations *Atmospheric Chemistry and Physics*, 16(24), 15605–15617. <https://doi.org/10.5194/acp-16-15605-2016>
- Larsen, N. K., Levy, L. B., Carlson, A. E., Buizert, C., Olsen, J., Strunk, A., ... Skov, D. S. (2018). Instability of the Northeast Greenland Ice Stream over the last 45,000 years. *Nature Communications*, 9(1), 1872. <https://doi.org/10.1038/s41467-018-04312-7>
- Leeson, A. A., Eastoe, E., & Fettweis, X. (2018). Extreme temperature events on Greenland in observations and the MAR regional climate model. *The Cryosphere*, 12(3), 1091–1102. <https://doi.org/10.5194/tc-12-1091-2018>
- Listowski, C., & Lachlan-Cope, T. (2017). The microphysics of clouds over the Antarctic Peninsula Part 2: modelling aspects within Polar WRF. *Atmospheric Chemistry and Physics*, 17(17), 10195-10221. <https://doi.org/10.5194/acp-17-10195-2017>
- Lo, J.C-F., Yang, Z-L. & Pielke Sr, R.A. (2008). Assessment of three dynamical climate downscaling methods using the Weather Research and Forecasting (WRF) model. *JGR: Atmospheres*. 113, D09112, <https://doi.org/10.1029/2007JD009216>
- Mayer, C., Schaffer, J., Hattermann, T., Floricioiu, D., Krieger, L., Dodd, P. A., ... Schannwell, C. (2018). Large ice loss variability at Nioghalvfjærdssjøen Glacier, Northeast Greenland. *Nature Communications*, 9(1), 2768. <https://doi.org/10.1038/s41467-018-05180-x>
- Mernild, S. H., Liston, G. E., van As, D., Hasholt, B., & Yde, J. C. (2018). High-resolution ice sheet surface mass-balance and spatiotemporal runoff simulations: Kangerlussuaq, west Greenland. *Arctic, Antarctic, and Alpine Research*, 50(1) S100008. <https://doi.org/10.1080/15230430.2017.1415856>
- Mottram, R., Boberg, F., Langen, P. ., Yang, S., Rodehacke, C., Christensen, J. ., & Madsen, M. (2017a). Surface mass balance of the Greenland ice sheet in the regional climate model HIRHAM5: Present state and future prospects. *Low Temperature Science*, 75, 105-115.
- Mottram, R., Nielsen, K.P., Gleeson, E., Yang, X. (2017b): Modelling Glaciers in the HARMONIE-AROME NWP model, *Adv. Sci. Res.*, 14, 323–334, <https://doi.org/10.5194/asr-14-323-2017>
- Mouginot, J., Rignot, E., Scheuchl, B., Fenty, I., Khazendar, A., Morlighem, M., ... Paden, J. (2015). Fast retreat of Zachariæ Isstrøm, northeast Greenland. *Science*, 350(6266), 1357-1361. <https://doi.org/10.1126/SCIENCE.AAC7111>
- Münchow, A., Schaffer, J. & Kanzow, T. (2019). Ocean circulation connecting Fram Strait to Glaciers off North-East Greenland: Mean flows, topographic Rossby waves, and their forcing. *J. of Physical Oceanography*, in press.
- Niwano, M., Aoki, T., Hashimoto, A., Matoba, S., Yamaguchi, S., Tanikawa, T., Fujita, K., Tsushima, A., Iizuka, Y., Shimada, R., and Hori, M. (2018.) NHM–SMAP: spatially and temporally high



resolution nonhydrostatic atmospheric model coupled with detailed snow process model for Greenland Ice Sheet, *The Cryosphere*, 12, 635–655, <https://doi.org/10.5194/tc-12-635-2018>

Noël, B., van de Berg, W. J., Machguth, H., Lhermitte, S., Howat, I., Fettweis, X., & van den Broeke, M. R. (2016). A daily, 1 km resolution data set of downscaled Greenland ice sheet surface mass balance (1958–2015). *The Cryosphere*, 10(5), 2361–2377. <https://doi.org/10.5194/tc-10-2361-2016>

Otte, T.L., Nolte, C.G., Otte, M.J. & Bowden, J.H. (2012). Does Nudging Squelch the Extremes in Regional climate modeling? *J. of Climate*, 25, 7046-7066, <https://doi.org/10.1175/JCLI-D-12-00048.1>

Pedersen, S.H., Tamstorf, M.P., Abermann, J., Westergaard-Nielsen, A., Lund, M... Schmidt, N.M. (2016). Spatiotemporal characteristics of seasonal snow cover in Northeast Greenland from in situ observations. *Arctic, Antarctic and Alpine Research*, 48 (4), 653–671. <https://doi.org/10.1657/AAAR0016-028>

Polar Weather Research and Forecasting Model, developed by Ohio State University, available from: <http://polarmet.osu.edu/PWRF/>, last accessed: July 29 2019.

Powers, J. G., Klemp, J. B., Skamarock, W. C., Davis, C. A., Dudhia, J., Gill, D. O., ... Duda, M. G. (2017). The Weather Research and Forecasting Model: Overview, System Efforts, and Future Directions. *Bulletin of the American Meteorological Society*, 98(8), 1717–1737. <https://doi.org/10.1175/BAMS-D-15-00308.1>

Rignot, E., Fenty, I., Xu, Y., Cai, C., & Kemp, C. (2015). Undercutting of marine-terminating glaciers in West Greenland *Geophysical Research Letters*, 42(14), 5909–5917. <https://doi.org/10.1002/2015GL064236>

Schaffer, J., von Appen, W.-J., Dodd, P. A., Hofstede, C., Mayer, C., de Steur, L., & Kanzow, T. (2017a). Warm water pathways toward Nioghalvfjærdsfjorden Glacier, Northeast Greenland. *Journal of Geophysical Research: Oceans*, 122(5), 4004–4020. <https://doi.org/10.1002/2016JC012462>

Sea Surface Temperature and Sea Ice Concentration Data, available from

<https://rda.ucar.edu/datasets/ds277.7/>, last accessed July 29 2019, doi:10.5065/EMOT-ID34

Shepherd, A., Ivins, E., Rignot, E... Wuite, J. (2019). Mass balance of the Greenland Ice Sheet from 1992 to 2018. *Nature*, in press. doi:10.1038/s41586-019-1855-2

Skamarock, W. C., & Klemp, J. B. (2008). A time-split nonhydrostatic atmospheric model for weather research and forecasting applications. *Journal of Computational Physics*, 227(7), 3465–3485. <https://doi.org/10.1016/j.jcp.2007.01.037>

Tedesco, M., Fettweis, X., Mote, T., Wahr, J., Alexander, P., Box, J. E., & Wouters, B. (2013). Evidence and analysis of 2012 Greenland records from spaceborne observations, a

- regional climate model and reanalysis data. *The Cryosphere*, 7(2), 615–630. <https://doi.org/10.5194/tc-7-615-2013>
- Turton, J. V., Mölg, T. & Van As, D. (2019a). Atmospheric Processes and Climatological Characteristics of the 79N Glacier (Northeast Greenland). *Monthly Weather Review*, 147(4), 1375–1394. <https://doi.org/10.1175/MWR-D-18-0366.1>
- Turton, J. V., Mölg, T & Collier, E. (2019b) NEGIS\_WRF model output, Open Science Framework Repository, last accessed October 1 2019, doi: /10.17605/OSF.IO/53E6Z.
- Van As, D., Boggild, C.E., Nielsen, S., Ahlstrom, A.P., Fausto, R.S., Podlech, S. & Andersen, M.L. (2009). Climatology and ablation at the South Greenland ice sheet margin from automatic weather station observations. *The Cryosphere Discussions*. 3, 117-158. <https://doi.org/10.5194/tcd-3-117-2009>
- van As, D., & Fausto, R. (2011). Programme for Monitoring of the Greenland Ice Sheet (PROMICE): first temperature and ablation records. *Geological Survey of Denmark and Greenland Bulletin*, 23, 73–76.
- van den Broeke, M., Box, J., Fettweis, X., Hanna, E., Noël, B., Tedesco, M., ... van Kampenhout, L. (2017). Greenland Ice Sheet Surface Mass Loss: Recent Developments in Observation and Modeling. *Current Climate Change Reports*, 3(4), 345–356. <https://doi.org/10.1007/s40641-017-0084-8>
- Wang, C., Graham, R.M., Wang, K., Gerland, S. & Granskog, M.A. (2019). Comparison of ERA5 and ERA-Interim near surface air temperature, snowfall and precipitation over Arctic sea ice: effects on sea ice thermodynamics and evolution. *The Cryosphere*, 13, 1661-1679, <https://doi.org/10.5194/tc-13-1661-2019>
- Weather Research and Forecasting Model, developed by the National Centre for Atmospheric Research (NCAR). Available from: <https://www.mmm.ucar.edu/weather-research-and-forecasting-model>, last accessed: October 1 2019.
- Wilson, A. B., Bromwich, D. H., & Hines, K. M. (2011). Evaluation of Polar WRF forecasts on the Arctic System Reanalysis domain: Surface and upper air analysis. *Journal of Geophysical Research*, 116(D11), D11112. <https://doi.org/10.1029/2010JD015013>